Adaptive Modulation and Coding for Free-Space Optical Channels

Ivan B. Djordjevic

***Abstract*—Adaptive modulation and coding can provide robust and spectrally efficient transmission over terrestrial free-space optical channels. Three adaptive modulation schemes are considered in this paper: (i) variable-rate variable-power adaptation, (ii) channel inversion, and (iii) truncated channel inversion schemes. It is shown that a simple channel inversion scheme performs comparable to a variable-rate variable-power adaptation scheme in the weak turbulence regime but faces significant performance degradation in the strong turbulence regime. We further study adaptive coding based on large-girth quasi-cyclic low-density parity-check- (LDPC-) coded modulation. It is shown by simulation that deep fades of the order of 30 dB and above in the regime of strong turbulence can be tolerated with the proposed scheme. It is demonstrated that communication in the saturation regime is possible with the proposed adaptive LDPC-coded modulation. We also determine the spectral efficiencies for the proposed adaptive modulation and adaptive coding schemes.**

***Index Terms*—Atmospheric turbulence; Adaptive modulation; Adaptive coding; Free-space optical (FSO) communications; Low-density parity-check (LDPC) codes**.

I. Introduction

Free-space optics (FSO) communication is a technology that can address any connectivity needs in future optical networks, be they in the core, edge, or access [1,2]. In metropolitan area networks (MANs), FSO can be used to extend the existing MAN rings; in enterprise, FSO can be used to enable local-area-network- (LAN-) to-LAN connectivity and intercampus connectivity; and FSO is an excellent candidate for last-mile connectivity [2]. However, an optical wave propagating through the atmosphere experiences fluctuations in amplitude and phase, known as scintillation, due to variations in the refractive index of the transmission medium because of inhomogenities in temperature and pressure caused by solar heating and wind. Scintillation represents one of the most important factors that degrade the performance of an FSO communication link that is present even under clear sky conditions. To deal with atmospheric turbulence, different coding approaches have been proposed including coded orthogonal frequency division multiplexing (OFDM) [3], coded multi-input multi-output (MIMO) [4], and so called rateless coding [5–8]. The key idea in the coded-OFDM approach is to lower the symbol rate by using OFDM and, in combination with interleaving and strong channel codes, to obtain high tolerance to the deep fades that are inherent to a turbulent channel. In a space–time coded-MIMO approach [4], M optical sources and N photodetectors are used to improve immunity to the atmospheric turbulence. In [7] code-rate adaptive codes [5,8] are advocated. In particular, the *raptor codes*, introduced by Shokrollahi in [6], obtained by concatenating an inner error-correcting code (the precode) with an outer fountain code such as a Luby-transform (LT) code, have been shown to provide high tolerance to deep fades due to atmospheric turbulence [7]. However, the achievable information rates (lower bounds on channel capacity) results [9] indicate that those approaches are still several decibels away from channel capacity, suggesting that there is still some room for improvement.

In this paper we propose to use adaptive modulation and coding as an efficient way to deal with strong atmospheric turbulence. Adaptive modulation and coding, already in use in wireless channels, enables robust and spectrally efficient transmission over time-varying channels [10–12]. The key idea behind our proposal is to estimate the channel conditions at the receiver side and feed this channel estimate back to the transmitter using an RF feedback channel, so that the transmitter can be adapted relative to the channel conditions. We study three different adaptive modulation scenarios: (i) variable-rate variable-power adaptation, (ii) channel inversion with a fixed rate, and (iii) truncated channel inversion with a fixed rate. We also study the improvements that can be obtained by using adaptive low-density-parity-check- (LDPC-) coded

Manuscript received March 6, 2009; revised March 16, 2010; accepted March 16, 2010; published April 13, 2010 (Doc. ID 110011).

I. B. Djordjevic (e-mail: ivan@ece.arizona.edu) is with the Department of Electrical and Computer Engineering, University of Arizona, Tucson, Arizona 85721, USA

Digital Object Identifier 10.1364/JOCN.2.000221

1943-0620/10/050221-9/$15.00

modulation. We show that in the strong turbulence regime, even deep fades of the order of 30 dB and above can be tolerated.

The paper is organized as follows. In Section II we describe the adaptive modulation and coding scheme with an RF feedback channel and channel model. In Section III we describe different adaptive modulation scenarios and determine the corresponding channel capacity. In Section IV we describe a particular adaptive coding scheme based on adaptive LDPC-coded modulation. In Section V some important concluding remarks are given.

II. Description of the Proposed FSO Communication System

The adaptive FSO communication system, shown in Fig. 1, consists of a transmitter, a propagation path through the atmosphere, and a receiver. The optical transmitter includes a semiconductor laser of high launch power, an adaptive modulation and coding block, and a power control block. To reduce the system cost, direct modulation of a laser diode is used.

The FSO system represents an intensity modulation with direct detection (IM/DD) system. The modulated beam is projected toward the distant receiver by using an expanding telescope assembly. Along the propagation path through the atmosphere, the light beam experiences absorption, scattering, and atmospheric turbulence, which cause attenuation, random variations in amplitude and phase, and beam wandering. At the receiver side, an optical system collects the incoming light and focuses it onto a detector, which generates an electrical current proportional to the incoming power. The intensity channel estimate is transmitted back to the transmitter by using an RF feedback channel. Because the atmospheric turbulence changes slowly, with correlation time ranging from 10 μs to 10 ms, this is a plausible scenario for FSO channels with data rates of the order of Gb/s. Notice that erbium-doped fiber amplifiers (EDFAs) cannot be used at all in this scenario because the fluorescence time is too long (about 10 ms). On the other hand, semiconductor optical amplifiers (SOAs) can be used if needed. In our study below we do not use any optical amplifier at all. Given the fact that systems integrating RF and FSO technologies have recently been reported in [13] (although for indoor applications) and the data rates needed for RF feedback are low, the proposed system is a promising candidate for future FSO systems. Notice that FSO systems have to use an RF backup channel to provide communication under severe weather conditions (such as fog). Therefore, the use of RF feedback does not introduce a significant system cost increase. Moreover, by taking into account the eye safety considerations and power efficiency, with power and rate adaptation we can avoid transmission at maximum laser power even when the atmospheric conditions are favorable and atmospheric turbulence is weak. Notice that the proposed adaptive modulation/coding scheme can also be used in indoor optical wireless links to deal with multipath interference.

The FSO communication channel model is described by

$$y_t = Ri_t x_t + n_t, \tag{1}$$

where $x=\{x_t\}_{t\geqslant 0}$ is the transmitted signal, $i=\{i_t\}_{t\geqslant 0}$ ($i_t \geqslant 0$) is the instantaneous intensity gain (irradiance), $y=\{y_t\}_{t\geqslant 0}$ is the received signal, $n=\{n_t\}_{t\geqslant 0}$ is the additive white Gaussian noise (AWGN) with a normal distribution $N(0,\sigma^2)$ representing the transimpedance amplifier thermal noise, and R denotes the p.i.n. photodiode responsivity. (Without the loss of generality in the rest of the paper we will set $R=1$ A/W.) Two important parameters in describing the effects of atmospheric turbulence are correlation length d_0 (d_0 is typically in the range of 1–10 cm) and correlation time τ_0 (τ_0 is typically 1–10 ms or longer) [1]. These two parameters are related by [1] $\tau_0 = d_0/v_\perp$, where $v_\perp$ is the wind velocity perpendicular to the propagation direction. Therefore, different techniques to deal with atmospheric turbulence can be classified as time domain and spatial domain. Since in the time domain it is quite challenging to deal with this affect, here we instead use spatial-domain techniques to deal with atmospheric turbulence, in particular spatial diversity. In the spatial-diversity technique, an array of M direct detection receivers can be used to deal with this problem as explained in [1] (see Fig. 11.15 on p. 466). By providing that the aperture diameter of each receiver is smaller than the spatial correlation width of the irradiance function, the array elements will be

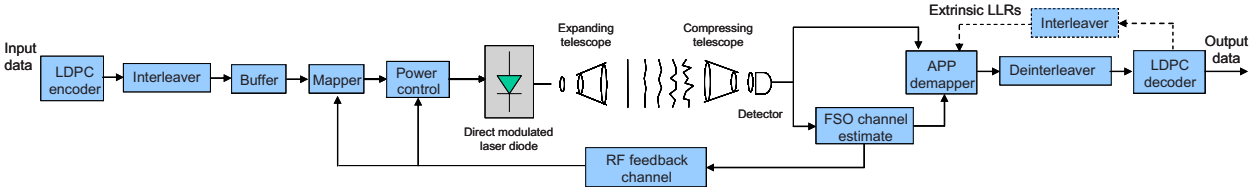

Fig. 1. (Color online) Block diagram of the adaptive modulation and coding terrestrial FSO system with RF feedback. LLRs, log-likelihood ratios; APP, *a posteriori* probability.

sufficiently separated so that they act independently. In that case, the summed output samples of the array will still be independent as shown in [1] (p. 469). [All signals in Eq. (1) are real valued.]

Several probability density functions (PDFs) have been proposed for the intensity variations at the receiver side of an FSO link [1]. For example, Al-Habash *et al.* [14] proposed a statistical model that factorizes the irradiance as the product of two independent random processes (large-scale and small-scale factors) each with a gamma PDF. It was shown in [1,7,9] that the predicted distribution matches very well the distributions obtained from numerical propagation simulations and experiments, and as such it is adopted here. The PDF of the intensity fluctuation is given by [14]

$$p(i_t) = \frac{2(\alpha\beta)^{(\alpha+\beta)/2}}{\Gamma(\alpha)\Gamma(\beta)} i_t^{(\alpha+\beta)/2-1} K_{\alpha-\beta}(2\sqrt{\alpha\beta i_t}), \quad i_t > 0, \tag{2}$$

where i_t ($t \geqslant 0$) is the signal intensity, α and β are parameters of the PDF, Γ is the gamma function, and $K_{\alpha-\beta}$ is the modified Bessel function of the second kind of order $\alpha-\beta$. The parameters α and β are related to the scintillation, and in the case of zero inner scale ($l_0=0$) (for plane waves) they are given by [1,14,15]

$$\alpha = \frac{1}{\exp\left[\dfrac{0.49\sigma_R^2}{(1+1.11\sigma_R^{12/5})^{7/6}}\right]-1}, \qquad \beta = \frac{1}{\exp\left[\dfrac{0.51\sigma_R^2}{(1+0.69\sigma_R^{12/5})^{5/6}}\right]-1}, \tag{3}$$

where ${\sigma_R}^2$ is the Rytov variance defined as

$$\sigma_R^2 = 1.23 C_n^2 k^{7/6} L^{11/6}, \tag{4}$$

where $k=2\pi/\lambda$ (λ is the wavelength), L denotes the propagation distance, and ${C_n}^2$ is the refractive index structure parameter. Weak fluctuations are associated with ${\sigma^2}_R<1$, moderate with ${\sigma^2}_R\approx 1$, strong with ${\sigma^2}_R>1$, and the saturation regime is defined by ${\sigma^2}_R\to\infty$ [1]. Notice that the summed output of an array of direct detection receivers still has gamma-gamma distribution, but with new parameters α and β as given below [1]:

$$\alpha_M = \frac{1+M\beta}{M\beta\sigma_I^2 - 1}, \quad \beta_M = M\beta, \tag{5}$$

where M is the number of detectors in the array and σ_I^2 is the scintillation index, defined as $\sigma_I^2 = E[i_t^2]/E^2[i_t]-1$ ($E[\ ]$ denotes the mathematical expectation operator).

Given this description of the system model and channel model, in the next two sections we describe our adaptive modulation/coding concept.

III. Adaptive Modulation

There are many parameters that can be varied at the transmitter side relative to the FSO channel intensity gain, including data rate, power, coding rate, and combinations of different adaptation parameters. The transmitter power adaptation, similar to wireless communications, can be used to compensate for the signal-to-noise ratio (SNR) variation due to atmospheric turbulence, with the aim to maintain a desired bit error rate (BER). The power adaptation therefore inverts the FSO channel scintillation so that the FSO channel behaves similarly to an AWGN channel to the receiver. In all simulation results in this paper, the spectral efficiencies are plotted against the average electrical SNR at the receiver, defined as $\mathrm{SNR}=PE[i_t^2]/\sigma^2$, where σ^2 is the variance of thermal noise and $P=E[x_t^2]$. Notice that this definition is used in [16] (see also in [4,9]) but is different from [1], where the SNR is defined as $E^2[i_t]/N_0 (N_0/2=\sigma^2)$, or [17], where it is defined as $P_o/\sigma (E[i_t]\leqslant P_o)$. We selected this definition (out of three definitions used in FSO communications) because no optical amplifier is used and to be consistent with the digital communications literature [18]. This definition emphasizes the role of the receiver since it operates in the thermal-noise-dominated scenario, and its performance is determined by the electrical current (obtained upon conversion from the optical to the electrical domain). Notice also that the average power of the optical signal $E[x_t]$ and the average power of the electrical current at the receiver side are connected by a simple relationship that will be provided later in this section. Moreover, the spectral efficiencies obtained by using the $E[x_t^2]\leqslant P$ constraint represent a lower bound for the $E[x_t]\leqslant P$ constraint because the set of input signals defined by the former constraint is the subset of that defined by the latter.

The power adaptation policy for FSO channel inversion is similar to that for wireless links [10–12] and is defined by $P(i_t)=C/i_t^2$, where $C=P/E[1/i_t^2]$ and $P(i_t)$ is the instantaneous power. The FSO channel, upon channel inversion, appears to the transmitter as a standard AWGN channel with $\mathrm{SNR}=\Gamma_0/E[1/i_t^2]$, where $\Gamma_0=E_s/N_0$ is the signal-to-noise ratio in the absence of scintillation, with E_s being the symbol energy and $N_0/2$ being the double-side power spectral density

of AWGN related to variance by $\sigma^2=N_0/2$. The channel inversion can be detrimental when $i_t \to 0$ because the factor $E[1/i_t^2]$ tends to infinity. To avoid this problem the *truncated channel inversion* policy from wireless communications [9–12] can be adopted, in which the channel inversion is performed only when the irradiance is above the certain threshold $i_{\text{tsh}}>0$; that is, $P(i_t)=C/i_t^2$ for $i_t \geq i_{\text{tsh}}$ (zero otherwise). The threshold irradiance is to be chosen in such a way to maximize the channel capacity [9–12].

In variable-rate adaptation, we change the signal constellation size for the fixed symbol rate depending on the FSO channel conditions. When the FSO channel conditions are favorable we increase the constellation size, we decrease it when channel conditions are not favorable, and we do not transmit at all when the intensity channel coefficients are below the irradiance threshold. The adaptive code rate adaptation was already considered in [7] and as such is not a subject of interest in this paper.

In the rest of this section, we apply the adaptation policies described above to the M-ary pulse-amplitude modulation (MPAM) format, which is selected because negative amplitude signals cannot be transmitted over FSO channels with direct detection. The M-ary quadrature-amplitude modulation (MQAM), commonly used in wireless communications, is not power efficient because it requires the addition of DC bias to convert negative amplitudes to positive ones and as such is not considered here. Notice that M-ary pulse-position modulation (MPPM) can also be used. Because MPPM is highly spectrally inefficient, we restrict our attention to MPAM. On–off keying (OOK), commonly used in practice, is a special case of MPAM and can be obtained by setting $M=2$. We describe below three different adaptation policies: (i) the adaptive-power adaptive-rate scheme, (ii) channel inversion with a fixed rate, and (iii) truncated channel inversion with a fixed rate.

Before we continue with the description of different adaptation policies, we have to derive a target bit error probability equation P_b for an AWGN channel. In MPAM the transmitted signal x takes values from the discrete set $X=\{0,d,\ldots,(M-1)d\}$ $(M \geq 2)$, where d is the Euclidean distance between two neighboring points. If all signal constellation points are equiprobable, the average signal energy is given by $E_s=E[x^2_t]=d^2(M-1)(2M-1)/6$, and it is related to the bit energy E_b by $E_s=E_b \log_2 M$, so that the signal-to-noise ratio per bit is defined by $SNR_b=E_b/N_0=E_S/(N_0 \log_2 M)=d^2(M-1)(2M-1)/(6N_0 \log_2 M)$. Because $E[x_t]=d(M-1)/2$ we can quite easily establish a connection between various SNR definitions.

Following the derivation in [10,18], we derive the following expression for bit error probability:

$$P_b \cong \frac{M-1}{M \log_2 M} \text{erfc}\left(\sqrt{\frac{3\Gamma_0}{2(M-1)(2M-1)}} \right), \quad (6)$$

where the symbol SNR Γ_0 was introduced earlier, and the erfc(z) function is defined by

$$\text{erfc}(z) = \frac{2}{\sqrt{\pi}} \int_z^\infty \exp(-u^2) \text{d}u.$$

Because Eq. (6) is not invertible with respect to the SNR, following a methodology similar to that introduced in [11], we derive the following empirical formula, which is valid in the regime of medium and high signal-to-noise ratios:

$$P_b \cong 0.2 \exp\left[-\frac{1.85\Gamma_0}{2^{2.19 \log_2 M}-1} \right]. \quad (7)$$

In Fig. 2 we illustrate the validity of empirical Eq. (7) (obtained by modifying the Chernoff bound) for different signal constellation sizes. For small constellations the agreement is very good with Monte Carlo simulations for all SNR values, whereas for large constellations the agreement is good for medium and high SNRs. From Eq. (7) we can easily determine the number of bits m carried per symbol as the function of bit error probability P_b:

$$m = \log_2 M = \frac{1}{2.19} \log_2(1+K\Gamma_0), \quad K = -\frac{1.85}{\ln(5P_b)}. \quad (8)$$

In the presence of atmospheric turbulence the number of bits per symbol becomes a function of FSO channel irradiance i_t as follows:

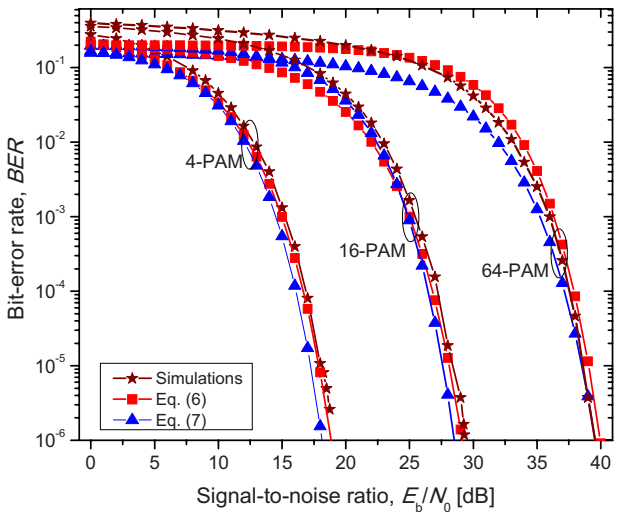

Fig. 2. (Color online) Bit error probability versus SNR per bit for MPAM on the AWGN channel.

$$m(i_t)=\frac{1}{2.19}\log_2\left[1+K\Gamma(i_t)\frac{P(i_t)}{P}\right],\quad \Gamma(i_t)=i_t^2\Gamma_0. \tag{9}$$

This equation can be used to adapt the signal constellation size depending on the FSO channel irradiance (i.e., to perform the rate adaptation). To derive the optimum power adaptation policy, we can define the Lagrangian (for more details on the Lagrangian multiplier method please see [10], Chapter 10)

$$L[P(i_t)]=\int_0^\infty m(i_t)p(i_t)\mathrm{d}i_t+\lambda\left[\int_0^\infty P(i_t)p(i_t)\mathrm{d}i_t-P\right], \tag{10}$$

where the $p(i_t)$ is the PDF of the irradiance given by Eq. (2). By differentiating the Lagrangian with respect to $P(i_t)$ and setting this derivative to be equal to zero we obtained the following *optimum power adaptation policy* (known as water filling in information theory [10] and wireless communications [11,12]):

$$\frac{K\Gamma_0P(i_t)}{P}=\begin{cases}\dfrac{1}{i_{\mathrm{tsh}}^2}-\dfrac{1}{i_t^2}, & i_t\geq i_{\mathrm{tsh}}\\ 0, & i_t<i_{\mathrm{tsh}}\end{cases}. \tag{11}$$

With this adaptation policy more power and higher data rates are transmitted when the FSO channel conditions are good, less power and lower data rates are transmitted when the FSO channel is bad, and nothing is transmitted when the FSO irradiance falls below the threshold i_{tsh}. By substituting Eq. (11) into $\int_{i_{\mathrm{ths}}}^\infty P(i_t)p(i_t)\mathrm{d}i_t=P$ we obtain

$$\int_{i_{\mathrm{tsh}}}^\infty\left(\frac{1}{i_{\mathrm{tsh}}^2}-\frac{1}{i_t^2}\right)p(i_t)\mathrm{d}i_t=K\Gamma_0. \tag{12}$$

The optimum threshold can be obtained numerically by solving Eq. (12).

The spectral efficiency, defined using the conventional definition from [18] (data rate R over channel bandwidth B), can be evaluated by substituting Eq. (11) into Eq. (9):

$$\frac{R}{B}=\frac{1}{2.19}\int_{i_{\mathrm{tsh}}}^\infty\log_2\left(\frac{i_t^2}{i_{\mathrm{tsh}}^2}\right)p(i_t)\mathrm{d}i_t\ [\mathrm{bits/s/Hz}]. \tag{13}$$

In Fig. 3 we show the spectral efficiencies [obtained using Eq. (13)] that can be achieved using power and rate adaptation and MPAM for different target bit error probabilities and both the weak turbulence regime ($\sigma_R=0.2$, $\alpha=51.913$, $\beta=49.113$) [Fig. 3(a)] and the strong turbulence regime ($\sigma_R=2$, $\alpha=4.3407$, $\beta=1.3088$) [Fig. 3(b)]. For example, the spectral efficiency R/B of 2 bits/s/Hz at $P_b=10^{-9}$ is achieved for a symbol SNR of 23.3 dB in the weak turbulence regime and 26.2 dB in the strong turbulence regime.

Although the adaptive-rate adaptive-power scheme

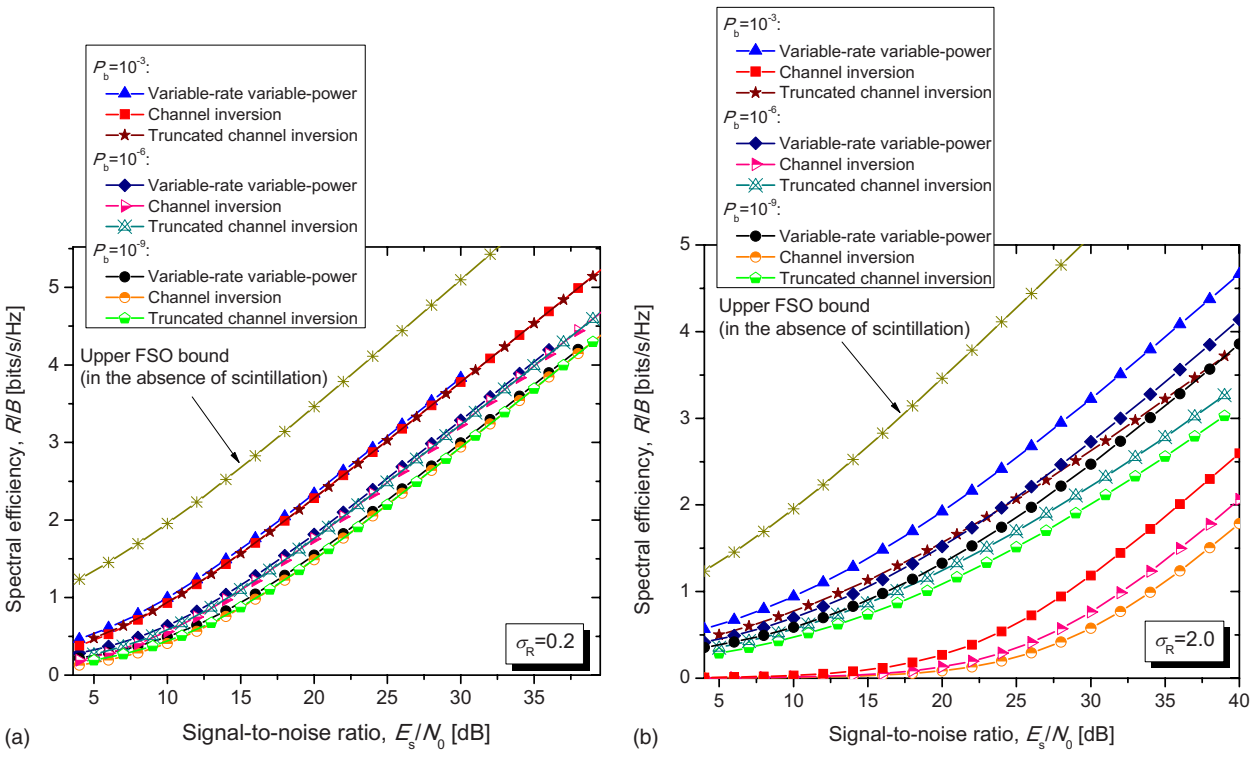

Fig. 3. (Color online) Spectral efficiencies against symbol SNR for different target bit probabilities of error: (a) in the weak turbulence regime and (b) in the strong turbulence regime.

is optimum, the threshold computation in Eq. (12) is time extensive. Instead, we can perform channel inversion with a fixed rate. The channel inversion adaptation can be performed by

$$\frac{P(i_t)}{P} = \frac{1}{i_t^2 E[1/i_t^2]}, \quad E[1/i_t^2] = \int_0^\infty \frac{1}{i_t^2} p(i_t) \mathrm{d}i_t. \tag{14}$$

To determine the spectral efficiency of the channel inversion scheme, we have to substitute Eq. (14) into Eq. (9) to obtain

$$\frac{R}{B} = \frac{1}{2.19} \log_2\left(1 + K\Gamma_0 \frac{1}{E[1/i_t^2]}\right). \tag{15}$$

In Fig. 3 we report the spectral efficiencies that can be achieved by employing this simple power adaptation scheme. Interestingly, in the weak turbulence regime [see Fig. 3(a)] this scheme performs comparably to the adaptive-power adaptive-rate scheme. However, in the strong turbulence regime [see Fig. 3(b)] this scheme faces significant performance degradation. Therefore, in the strong turbulence regime we have to employ the truncated channel inversion scheme, instead.

In truncated channel inversion we perform the following power adaptation:

$$\frac{P(i_t)}{P} = \begin{cases} \dfrac{1}{i_t^2 E_{i_{\mathrm{tsh}}}[1/i_t^2]}, & i \geqslant i_{\mathrm{tsh}} \\ 0, & i < i_{\mathrm{tsh}} \end{cases},$$

$$E_{i_{\mathrm{tsh}}}[1/i_t^2] = \int_{i_{\mathrm{tsh}}}^\infty \frac{1}{i_t^2} p(i_t) \mathrm{d}i_t. \tag{16}$$

The threshold i_{tsh} in Eq. (16) can be chosen to maximize the spectral efficiency in Eq. (15) with respect to threshold. The corresponding spectral efficiency expression is then given by

$$\frac{R}{B} = \frac{1}{2.19} \max_{i_{\mathrm{tsh}}} \left\{ \log_2\left(1 + K\Gamma_0 \frac{1}{E_{i_{\mathrm{tsh}}}[1/i_t^2]}\right) P(i_t \geqslant i_{\mathrm{tsh}}) \right\}, \tag{17}$$

where

$$P(i_t \geqslant i_{\mathrm{tsh}}) = \int_{i_{\mathrm{tsh}}}^\infty p(i_t) \mathrm{d}(i_t).$$

This maximization can be performed by the Monte Carlo integration approach, which is numerically less intensive than the numerical optimization in Eq. (12). For example, to evaluate $E_{i_{\mathrm{tsh}}}[i_t^{-2}]$ by Monte Carlo integration we have to perform the averaging of i_t^{-2} for intensity samples larger than threshold intensity.

In Fig. 3 we also report the spectral efficiencies that can be achieved by employing the truncated channel inversion. This scheme performs comparably to the adaptive-power adaptive-rate scheme in the weak turbulence regime, whereas at $P_b = 10^{-9}$ and for a spectral efficiency of 2 bits/s/Hz it performs 3.7 dB worse but significantly better than the simple channel inversion scheme.

In Fig. 4 we show the BER performance of uncoded nonadaptive MPAM for different turbulence strengths. In the weak turbulence regime, the BER performance loss is small. However, in the strong turbulence regime the BER performance degradation is large. The optimum adaptation policy at $P_b = 10^{-6}$ for a spectral efficiency of 4 bits/s/Hz (see Fig. 3) provides a moderate improvement of 3.3 dB in the weak turbulence regime, whereas the improvement in the strong turbulence regime is significant at 31.7 dB. Notice that spectral efficiencies are shown against symbol SNR, whereas the BERs in Figs. 4 and 5 are shown against the bit SNR so that modulation formats with different constellation sizes can be compared. This is a common practice in the digital communication literature (see [1,11,19]).

In this section we described three different adaptive modulation scenarios by employing uncoded MPAM. In the next section we describe the adaptive coding based on LDPC-coded MPAM.

IV. Adaptive LDPC-Coded Modulation

By using the trellis-coded modulation (TCM), introduced by Ungerboeck [20], in combination with convolutional codes or by using coset codes, introduced by Forney [21], in combination with block codes, we can separate the encoding and modulation process (see

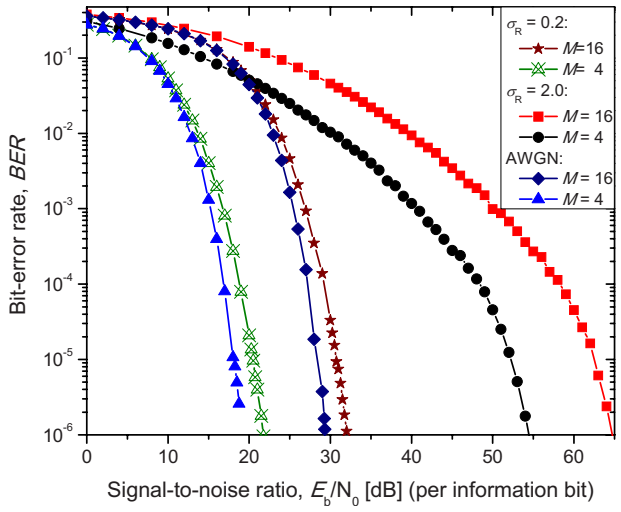

Fig. 4. (Color online) Nonadaptive uncoded MPAM bit error probabilities against bit SNR.

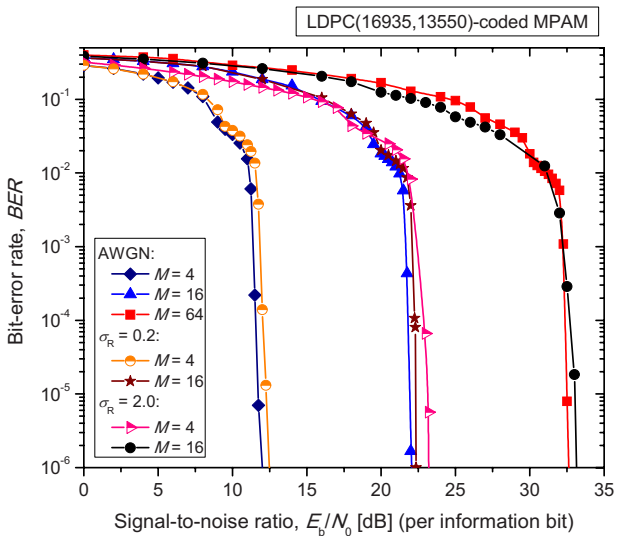

Fig. 5. (Color online) Nonadaptive LDPC-coded bit error probabilities versus SNR per bit for MPAM on the AWGN channel, under the weak turbulence regime and under the strong turbulence regime.

[11,12] for more details). However, to keep the complexity of this approach reasonably low the convolutional or block codes should be simple and short. Those codes are low rate and weak so that coding gains are moderate. For example, the adaptive coding scheme based on TCM proposed in [12] is about 5 dB away from channel capacity. Instead, in this paper we propose to implement adaptive coding based on LDPC-coded modulation. The input data are LDPC encoded and written to a buffer. Based on FSO channel irradiance, i_t, $m(i_t)$ bits are taken at a time from a *buffer* and used to select the corresponding point from the MPAM signal constellation. The number of bits to be taken from the buffer are determined by one of three methods described in Section III. The corresponding expressions for adaptation are to be modified to include the coding gain G_c of the LDPC code. Because the coding gain refers to the savings attainable in the energy required to achieve a given bit error probability when coding is used compared with that with no coding, the bit error probability of the LDPC-coded scheme can be evaluated by

$$P_b \cong 0.2 \exp\left[-\frac{1.85 G_c \Gamma_0}{2^{2.19 \log_2 M} - 1}\right]. \tag{18}$$

Therefore, all expressions derived in the previous section should be modified by substituting K with KG_c.

To facilitate the implementation at high speed we employ the quasi-cyclic LDPC codes [22,23] of girth 10. The parity-check matrix of quasi-cyclic LDPC codes can be written as follows:

$$H = \begin{bmatrix} I & I & I & \cdots & I \\ I & P^{S[1]} & P^{S[2]} & \cdots & P^{S[c-1]} \\ I & P^{2S[1]} & P^{2S[2]} & \cdots & P^{2S[c-1]} \\ \cdots & \cdots & \cdots & \cdots & \cdots \\ I & P^{(r-1)S[1]} & P^{(r-1)S[2]} & \cdots & P^{(r-1)S[c-1]} \end{bmatrix}, \tag{19}$$

where I is a $p \times p$ identity matrix, P is $p \times p$ permutation matrix (whose elements $p_{i,i+1}=p_{p,1}=1$, $i=1,2,\ldots,p-1$; other elements of P are zeros), and r and c represent the number of block rows and block columns in Eq. (19), respectively. p is a prime number. The set of integers S are to be chosen from the set $\{0,1,\ldots,p-1\}$ in such a way that cycles of short length in the corresponding bipartite graph representation of the H matrix are avoided. For example, for $p=1123$ and $S=\{0,2,5,13,20,37,58,91,135,160,220,292,354,712,830\}$ [from Eq. (19)] we obtain an LDPC code of rate 0.8, girth $g=10$, column weight 3, and length $N=16{,}845$. The soft iterative decoding of LDPC codes considered in this paper is based on the sum-product-with-correction-term algorithm [24].

In Fig. 5 we show the BER performance of nonadaptive LDPC(16935,13550)-coded MPAM for the AWGN channel, under the weak turbulence regime ($\sigma_R=0.2$), and under the strong turbulence regime ($\sigma_R=2.0$). In the weak turbulence regime the BER performance degradation is small, within 0.5 dB, whereas in the strong turbulence regime the BER performance degradation is so high that the adaptive coding approach described above is a necessity. The results of simulations are obtained for 25 LDPC decoder iterations and 3 LDPC decoder–APP demapper iterations. The gray mapping rule is used in simulations.

In Fig. 6 we show the spectral efficiency performance of adaptive LDPC(16935,13550)-coded MPAM for different adaptation scenarios. Given the fact that the channel capacity of the FSO channel under atmospheric turbulence is an open problem, we show in the same figure an upper bound in the absence of atmospheric turbulence (denoted in Fig. 6 as the upper FSO bound) from [25].

The coding gain over adaptive modulation at $P_b=10^{-6}$ for $R/B=4$ bits/s/Hz is 7.2 dB in both (weak and strong) turbulence regimes (see Figs. 3 and 6 at a spectral efficiency of 4 bits/s/Hz). Larger coding gains are expected at lower BERs and for higher spectral efficiencies. Further improvements can be obtained by increasing the girth of the LDPC codes and employing better modulation formats. The increase in codeword length to 100,515 does not improve the R/B performance that much, as shown in Fig. 6. It is interesting to notice that by employing adaptive coding, the communication under saturation regime is possible, as

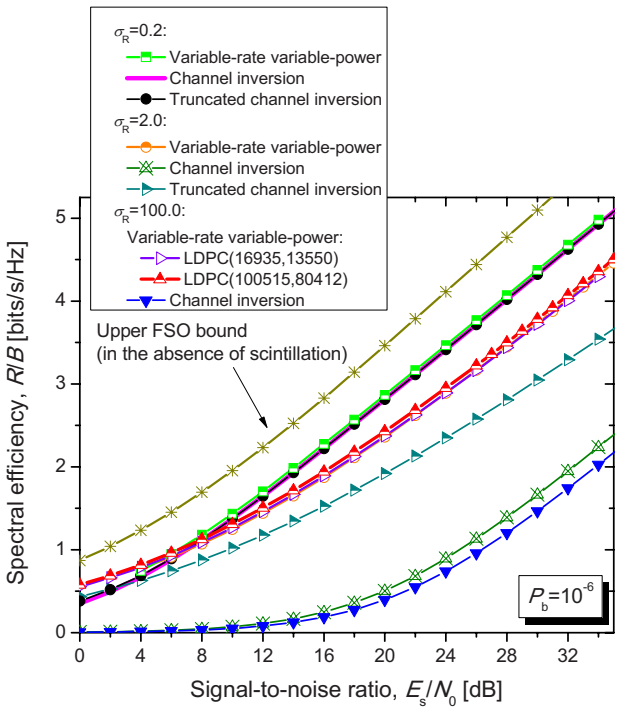

Fig. 6. (Color online) Spectral efficiencies against symbol SNR for adaptive LDPC-coded MPAM.

shown in Fig. 6. Moreover, for the variable-rate variable-power scheme there is no degradation in the saturation regime compared with the strong turbulence regime, whereas a small degradation was found for the channel inversion scheme. Overall improvement from adaptive modulation and coding for $R/B=4$ bits/s/Hz at $P_b=10^{-6}$ over nonadaptive uncoded modulation ranges from 10.5 dB (3.3 dB from adaptive modulation and 7.2 dB from coding) in the weak turbulence regime to 38.9 dB in the strong turbulence regime (31.7 dB from adaptive modulation and 7.2 dB from coding), which is significantly higher than that reported in [3,4,7], where improvements up to 25 dBs are reported.

Notice that results corresponding to OOK, which is commonly used in practice, can be obtained by setting $M=2$. From the numerical results reported in [15] (see Fig. 3), we conclude that in the strong turbulence regime the required SNR for OOK without adaptation to achieve a spectral efficiency of 1 bit/s/Hz is above 50 dB, which is difficult to satisfy in practice. Therefore, to enable communication under the strong turbulence regime the power and/or rate adaptation is unavoidable. Since soft decoding is used in the proposed scheme, the receiver complexity of MPAM is comparable to that of OOK.

V. Conclusion

We have described three adaptive modulation and adaptive coding schemes with RF feedback, which provide robust and spectrally efficient transmission over free-space optical channels, namely, (i) the variable-rate variable-power adaptation scheme, (ii) the channel inversion with a fixed rate scheme, and (iii) the truncated channel inversion scheme. It was demonstrated that the simple channel inversion scheme is sufficient in the weak turbulence regime. The use of either the variable-rate variable-power scheme or truncated channel inversion is needed in the strong turbulence regime. We also describe the adaptive LDPC-coded modulation scheme, which is able to tolerate deep fades of the order of 30 dB and above (at $P_b=10^{-6}$, $R/B=4$ bits/s/Hz) in the strong turbulence regime. With the proposed adaptive coding scheme even communication in the saturation regime is possible. Finally, we report the spectral efficiencies for the proposed adaptive modulation and adaptive coding schemes.

Topics of interest in future research include (i) determination of improvements in FSO channels when channel state information (CSI), provided by RF feedback, is imperfect and (ii) estimation of degradation due to delay in delivery of CSI to the transmitter.

Acknowledgments

This paper was supported in part by the National Science Foundation (NSF) under grant IHCS-0725405.

References

[1] L. C. Andrews and R. L. Philips, *Laser Beam Propagation Through Random Media*, SPIE Press, 2005.
[2] H. Willebrand and B. S. Ghuman, *Free-Space Optics: Enabling Optical Connectivity in Today's Networks*, Sams Publishing, 2002.
[3] I. B. Djordjevic, B. Vasic, and M. A. Neifeld, "LDPC coded OFDM over the atmospheric turbulence channel," *Opt. Express*, vol. 15, no. 10, pp. 6332–6346, May 2007.
[4] I. B. Djordjevic, S. Denic, J. Anguita, B. Vasic, and M. A. Neifeld, "LDPC-coded MIMO optical communication over the atmospheric turbulence channel," *J. Lightwave Technol.*, vol. 26, no. 5, pp. 478–487, Mar. 2008.
[5] M. Luby, "LT codes," *Proc. IEEE Symp. on Foundations of Computer Science (FOCS02)*, 2002, p. 43.
[6] A. Shokrollahi, "Raptor codes," *IEEE Trans. Inf. Theory*, vol. 52, pp. 2551–2567, June 2006.
[7] J. A. Anguita, M. A. Neifeld, B. Hildner, and B. Vasic, "Rateless coding on experimental temporally correlated FSO channels," *J. Lightwave Technol.*, vol. 28, no. 7, pp. 990–1002, Apr. 2010.
[8] D. J. C. MacKay, "Fountain codes," *IEE Proc.-Commun.*, vol. 152, pp. 1062–1068, Dec. 2005.
[9] S. Denic, I. B. Djordjevic, J. Anguita, B. Vasic, and M. A. Neifeld, "Information theoretic limits for free-space optical channels with and without memory," *J. Lightwave Technol.*, vol. 26, no. 19, pp. 3376–3384, Oct. 2008.
[10] T. M. Cover and J. A. Thomas, *Elements of Information Theory*, New York: Wiley, 1991.
[11] A. Goldsmith, *Wireless Communications*, Cambridge: Cambridge U. Press, 2005.
[12] A. Goldsmith and S.-G. Chua, "Adaptive coded modulation for

fading channels," *IEEE Trans. Commun.*, vol. 46, pp. 595–601, May 1998.

[13] J. Liao, S. Deng, K. Connor, and Z. R. Huang, "Antenna integration with laser diodes and photodetectors for a miniaturized dual-mode wireless transceiver," in *Proc. 58th Electronic Component Technology Conf. (ECTC)*, Orlando, FL, May 2008, pp. 1864–1868.

[14] M. A. Al-Habash, L. C. Andrews, and R. L. Phillips, "Mathematical model for the irradiance probability density function of a laser beam propagating through turbulent media," *Opt. Eng. (Bellingham)*, vol. 40, pp. 1554–1562, 2001.

[15] J. A. Anguita, I. B. Djordjevic, M. A. Neifeld, and B. V. Vasic, "Shannon capacities and error-correction codes for optical atmospheric turbulent channels," *BioInterphases*, vol. 4, no. 9, pp. 586–601, Sept. 2005.

[16] J. Li and M. Uysal, "Optical wireless communications: system model, capacity and coding," in *Proc. 2003 58th IEEE Vehicular Technology Conf.*, Oct. 2003, vol. 1, pp. 168–172.

[17] S. Hranilovic and F. R. Kschischang, "Capacity bounds for power- and band-limited optical intensity channels corrupted by Gaussian noise," *IEEE Trans. Inf. Theory*, vol. 50, no. 5, pp. 784–795, May 2004.

[18] J. G. Proakis, *Digital Communications*, Boston, MA: McGraw-Hill, 2001.

[19] J. G. Proakis, *Digital Communications*, Boston: McGraw-Hill, 2001.

[20] G. Ungerboeck, "Channel coding with multilevel/phase signals," *IEEE Trans. Inf. Theory*, vol. 28, pp. 55–67, Jan. 1982.

[21] G. D. Forney, Jr., "Coset codes—Part I: introduction and geometrical classification," *IEEE Trans. Inf. Theory*, vol. 34, pp. 1123–1151, Sept. 1988.

[22] M. P. C. Fossorier, "Quasi-cyclic low-density parity-check codes from circulant permutation matrices," *IEEE Trans. Inf. Theory*, vol. 50, pp. 1788–1794, Aug. 2004.

[23] I. B. Djordjevic, L. Xu, T. Wang, and M. Cvijetic, "Large girth low-density parity-check codes for long-haul high-speed optical communications," in *Proc. OFC/NFOEC 2008*, San Diego, CA, Feb. 2008, paper JWA53.

[24] X.-Y. Hu, E. Eleftheriou, D.-M. Arnold, and A. Dholakia, "Efficient implementations of the sum-product algorithm for decoding of LDPC codes," in *Proc. IEEE GLOBECOM*, vol. 2, Nov. 2001, pp. 1036–1036E.

[25] A. A. Farid and S. Hranilovic, "Upper and lower bounds on the capacity of wireless optical intensity channels," in *Proc. ISIT 2007*, Nice, France, June 2007, pp. 2416–2420.